Indian J. Phys. **68A** (1), 33 – 43 (1994)

I J P A
— an international journal

A Monte Carlo simulation of semiconductor detectors

T Pal, S L Sharma and H N Acharya

Department of Physics and Meteorology, Indian Institute of Technology, Kharagpur-721 302, West Bengal, India

Received 4 February 1993, accepted 18 August 1993

Abstract : A Monte-Carlo simulation algorithm has been developed to predict the response of semiconductor detectors to X- and γ-rays. The algorithm has been successfully applied to simulate the performance of α-HgI_2 detectors. The simulated results match very well with the reported experimental results.

Keywords : Monte-Carlo simulation algorithm, random selection, semiconductor detector, pulse height spectrum.

PACS Nos. : 02.60.Cb, 61.43.Bn, 29.40.Wk

1. Introduction

Often X-ray and γ-ray spectroscopy require detectors with high efficiency as well as high energy resolution. Silicon and germanium are the first materials used as X-ray and γ-ray detectors. Although these materials show excellent energy resolution, their low efficiencies and the need of refrigeration often make their application difficult. The search for suitable room-temperature operable X- and γ-ray semiconductor detectors has led to the development of detectors of three high-Z semiconducting materials [1], namely, gallium arsenide (GaAs), cadmium telluride (CdTe) and red mercuric iodide (α-HgI_2). Among these, however, red mercuric iodide has been found to be the most suitable.

It is known that thin detectors show good energy resolution, but suffer from poor efficiency. On the other hand, thick detectors have high efficiency but they show very poor resolution. So according to the demand of application, the optimization of the detector geometry, especially for high-Z semiconductor detectors, is very much required.

Although the physical effects occurring within the semiconductor detectors are separately well understood, it is not always clear exactly how the effects combine together to

produce complicated pulse height spectra in the laboratory. A useful tool to study this is a computerized simulation of the detector. Reliable simulation algorithms also can be used to optimize detector geometry and configuration, significantly reducing the experimental efforts usually associated with detector development.

In this paper, we present a Monte Carlo simulation algorithm to predict the response of semiconductor detectors. The algorithm has been successfully applied to α-HgI_2 semiconductor detectors.

2. Computational model

The problem of determining the response of a semiconductor radiation detector to X- and γ-rays can be divided into two parts : (a) transport of radiation through the detector medium and (b) creation and collection of the charge-carriers and subsequent pulse processing. Monte Carlo method, used in the present simulation of spectral response of semiconductor detectors, employs a two dimensional model for the transport of radiation through the medium and a one dimensional model for the collection of charge-carriers under a uniform electric field.

(a) Transport of radiation through the detector medium :

Radiation (X- or γ-ray) emitted from a source enters the detector, diffuses through it and is either absorbed in the medium or escapes from it through one of the bounding surfaces of the detector. Secondary radiations created directly or indirectly by the source radiations, in the process of interactions within the detector medium, also contribute to the transport problem.

In the present calculation, the source is considered to be an isotropic point source of zero thickness located on the axis of a cylindrical shaped detector. A coordinate system is set so that the detector axis lies along the z-axis and the origin lies on the front face of the detector

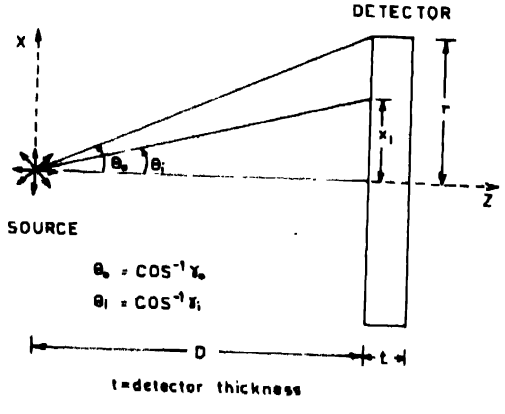

Figure 1. The source-detector geometry.

(Figure 1). The direction cosines (γ) of incident photons with respect to the z-axis are selected randomly from the following probability distribution [2] :

$$p(\gamma) = 1/(1-\gamma_0); \qquad \gamma_0 \leq \gamma \leq 1 \tag{1}$$

where γ_0 is the minimum value of the direction cosine. So the direction cosine of the i-th incidenting photon is given by :

$$\gamma_i = (1-\gamma_0)(i-R_i)N^{-1} + \gamma_0; \qquad i = 1, 2, 3,.....N \tag{2}$$

where N denotes the total number of source photons and R_i's are the random numbers between 0 and 1. There is no need to obtain the azimuthal angle for the source photons because of the assumed azimuthal symmetry. In all cases it is sufficient to allow the i-th source photon to intercept the detector along the X-axis at the position :

$$x_i = D\gamma_i^{-1}\left(1-\gamma_i^2\right)^{1/2}; \quad y_i = 0 \text{ and } z_i = 0 \tag{3}$$

where D is the source-detector separation distance.

The free paths of the photons in the detector medium are selected randomly as :

$$X_i = -1/\mu \ln R_i \tag{4}$$

where μ is the total attenuation coefficient of the detector material. If this selected distance carries a photon out of the detector medium, it is considered to be lost.

In the present calculation, photon energies below 1 MeV are considered. So, for calculating the interaction cross sections and the attenuation coefficients, only photoelectric effect and Compton scattering are taken into account. The mode of interaction is selected according to the flowchart given in Figure 2. In the case of detectors made up of compound semiconductors, the interacting atom is selected in the same fashion.

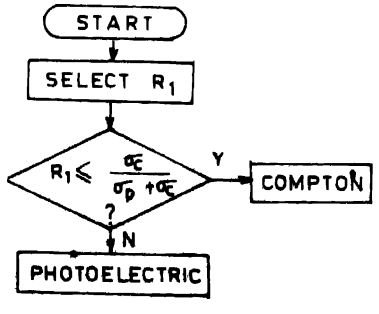

Figure 2. Flowchart showing the procedure for selecting the mode of interaction.

For photoelectric effect, K, L_I, L_{II}, L_{III} and an average value of M shell binding energies are considered. Flight angles (θ) of the photoelectrons with respect to the z-axis are randomly selected from the following probability distribution [3] :

$$p(\theta) = \frac{1}{\sigma_p}\frac{d\sigma_p}{d\theta} = \frac{3}{4}\frac{\sin^3\theta}{(1-\beta\cos\theta)^4}; \quad \beta = v/c. \tag{5}$$

Secondary X-ray emissions from K and L shells are taken into account according to the fluorescence yields [4] :

$$\omega_j = \left(1+a_j Z^{-4}\right)^{-1}; j = K, L; a_k \equiv 1.12\times10^6 \text{ and } a_L \equiv 6.4\times10^7 \tag{6}$$

Auger electrons with emission probability $\left(1 - \omega_j\right)$ are considered to be absorbed in the medium.

The application of rejection sampling technique' [5] to the Compton scattering cross section allows us to calculate the scattered photon energy and the angle of scattering. The differential cross section is given by Klein-Nishina formula :

$$\frac{d\sigma_c}{d\gamma_s} = 2\pi r_0^2 \left(\frac{\alpha'}{\alpha}\right)^2 \left[\frac{\alpha'}{\alpha} + \frac{\alpha}{\alpha} - 1 + \gamma_s^2\right] \tag{7}$$

where σ_c = the Compton cross section,

γ_s = the cosine of the angle of scattering,

r_0 = the classical electron radius,

α = the energy of the incident photon and

α' = the energy of the Compton photon.

The paths of the photoelectrons, Compton electrons and Auger electrons in the medium are considered to be straight lines. The energy deposited by the electrons along their paths in the detector medium is determined by calculating the stopping power of the material according to the relationship [6] :

$$-\frac{dE}{dx} = 0.153\frac{\rho Z}{A\beta^2}\left[\ln\frac{E\left(E+mc^2\right)^2\beta^2}{2I^2mc^2} + F(\beta)\right] \text{ MeV/cm},$$

$$F(\beta) = 1 - \beta^2 - \ln 2\left(2\sqrt{1-\beta^2} - 1 + \beta^2\right) \tag{8}$$

where E = the electron kinetic energy in keV,

ρ = the density of the material,

Z = the atomic number,

A = the mass number and

I = the ionization potential of the material.

In the present computational model, a single photon is considered at a time. The original photon as well as the secondary photons, produced by the original photon through photoelectric and Compton interactions are traced individually throughout in the detector medium. The extent of cascade is restricted, however, by terminating the branches whenever photon escapes from the detector or photon energy is degraded below the average M shell binding energy.

(b) Charge carrier transport :

For this, the detector is assumed to be a stack of thousand parallel slabs which are perpendicular to the detector axis. Energy deposited by the energetic electrons in each slab is calculated according to eq. (8). The number of electron-hole pairs generated in each slab is determined using the relation :

$$\bar{N} = \Delta E/w \tag{9}$$

where $\bar{N}$ = the average number of charge carrier pairs generated,

ΔE = the energy deposited in the particular slab and

w = the charge carrier pair creation energy.

$\bar{N}$ is subjected to a gaussian fluctuation with mean $\bar{N}$ and variance $\bar{N}F$, where F is the Fano factor. The induced charge on the electrode due to the charge carriers in a particular slab is given by [7] :

$$Q = Ne/d\left[(d-x) + L_h\left(1 - e^{-x/L_h}\right)\right]; \quad L_h = \mu_h \tau_h \varepsilon \tag{10}$$

where N = the number of charge carrier pairs generated,

e = the electronic charge,

d = the detector thickness,

x = the distance of the slab from the cathode,

L_h = the hole-trapping length,

μ_h = the hole mobility,

τ_h = the hole life-time and

ε = the applied electric field.

Once the total charge induced on the electrode for a single source photon is calculated, the final charge pulse is shaped by a simulated electronic circuit with differentiation and integration time constants of 4 μs. The two time constants are taken to be equal to maximize the signal to noise ratio. To meet the practical situation, an additional noise is added intentionally to each shaped pulse. This is done by subjecting the pulse to a gaussian fluctuation with a variance $\Delta E/2.355$ [8], where ΔE is the electronic noise. Finally, the pulse

output is analyzed with the help of a simulated multichannel analyzer. According to the height of the pulse, the count in one of the channels is increased by one. Thus all the generated pulses are analyzed and then the counts per channel versus channel numbers are strored in a suitable array. This array is the final output of the whole calculation. A simple histogram plot of this array represents the energy spectrum of the source photons.

3. Computer program

Flowchart of the program is shown in Figure 3. The present program is written in standard pascal programming language and consists of 589 lines. It was run on a Apollo Super Domain 10000 computer. Average CPU time required for running the program depends on

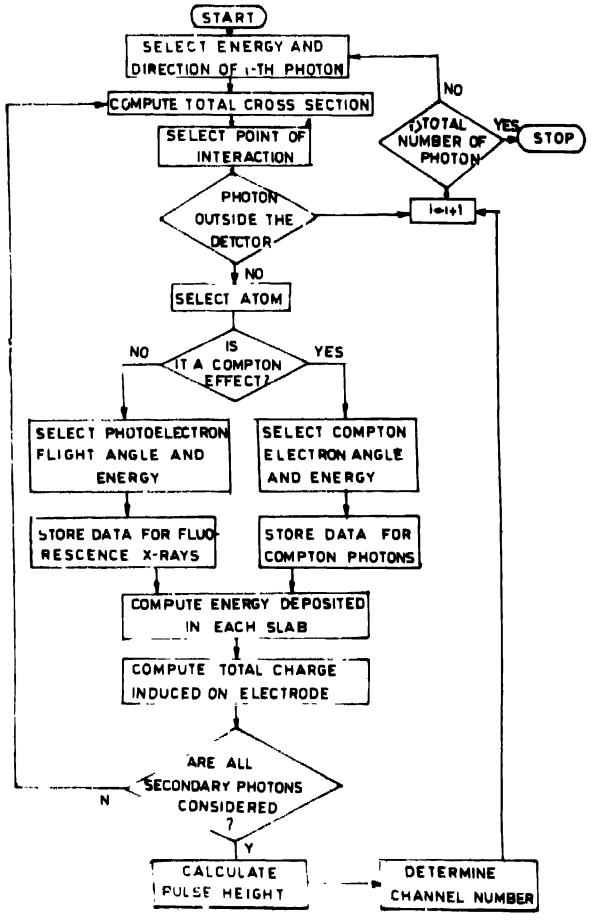

Figure 3. Flowchart of the simulation program.

the number of source photons and their energies. For ^{241}Am source (which has five photon energies) with 10^5 photons, the program takes about 5 minutes of CPU time. Table 1 lists the input parameters to the program.

4. Results and discussion

The simulations in this study are carried out for detector geometries commonly used in the laboratory. We present here the results obtained for α-HgI_2 detectors only.

Table 1. List of input parameters to the program.

Detector	:	Name of the detector. The following parameters for α-HgI_2 detectors are set by the program itself when the detector name is input :	
		Z1, Z2 (atomic numbers)	= 80, 53
		RHO1, RHO2 (atomic densities)	= 8.5×10^{21}, 1.69×10^{22}
		A_WEIGHT1, A_WEIGHT2 (atomic weights)	= 203, 127
		E_BK1, E_BK2 (K-shell B.E's in keV)	= 83.1, 33.17
		E_BL1i, E_BL1ii, E_BL1iii (L-shell B.E's for Hg in keV)	= 14.86, 14.2, 12.3
		E_BL2i, E_BL2ii, E_BL2iii (L-shell B.E's for I in keV)	= 5.2, 4.85, 4.56
		E_BM1, E_BM2 (average M-shell B.E's)	= 2.87 keV, 862 eV
		E_MOB (electron mobility)	= 100 cm^2/V-sec
		H_MOB (hole mobility)	= 4 cm^2/V-sec
		E_TR_TIME (electron trapping time)	= 4μs
		H_TR_TIME (hole trapping time)	= 0.75 μs
		EHPE (carrier pair creation energy)	= 4.15 eV
DET_THICK	:	Detector thickness	
DET_RAD	:	Detector radius	
SO_DET_DIST	:	Source-detector distance	
PHOTON	:	photon energies (Maximum 20 energies are allowed)	
PHO_NO	:	Number of photons emitting from the source with a particular energy (Maximum 214, 74, 82, 752 photons are allowed)	
BIAS	:	Detector bias voltage	
WIN	:	Channel window width	
NOISE	:	Electronic noise which is to be incorporated along with the signal	

Figure 4 shows the detection efficiencies (defined as the ratio of number of the interacting photons to the number of incident photons) at different photon energies for detectors having radius 0.25 cm and thicknesses 0.010, 0.025, 0.050 and 0.100 cm. Figure 5 shows the full energy peak efficiencies (defined as the ratio of the number of photons

depositing their energy fully in the detector medium to the number of incident photons) at different energies for the same detector thickness. Both these efficiencies increase with the increase of detector thickness.

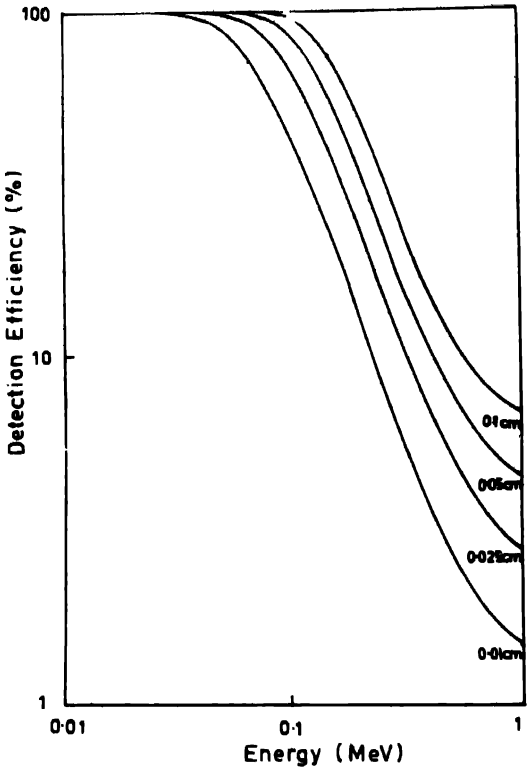

Figure 4. The detection efficiency *versus* energy curves for α-HgI_2 detectors of different thicknesses.

Figure 6 shows the spectral response for α-HgI_2 detectors of thicknesses 0.010, 0.025, 0.075 and 0.100 cm when ^{241}Am source is used. For the sake of comparison, experimental data obtained from ref. [9] for a 500 μm thick α-HgI_2 detector is superposed on Figure 6(c). Clearly, the simulated spectra very closely match with the experimental spectrum except at lower energies. There seems to be two possible reasons for this difference : the omission of charge-carrier detrapping effect and the effect of scattering of γ-rays from the nearby objects (backscatter). The backscattered photons would enhance the low energy region of the pulse height spectrum.

The existence of a peak at 31 keV in the simulated spectra and in the experimental spectrum clearly shows the effect of fluorescence X-ray escape. It is very interesting to note that, as the detector thickness increases, the 59 54 keV photopeak height increases and the 31 keV fluorescence X-ray escape peak height decreases. This is so because the full energy peak

efficiency increases with the detector thickness, which is also clearly seen in Figure 5. The tail in the 59.54 keV photopeak for thicker detectors shows the effect of hole trapping. Whereas, for thin detectors this effect is more or less totally absent. This is because of the fact

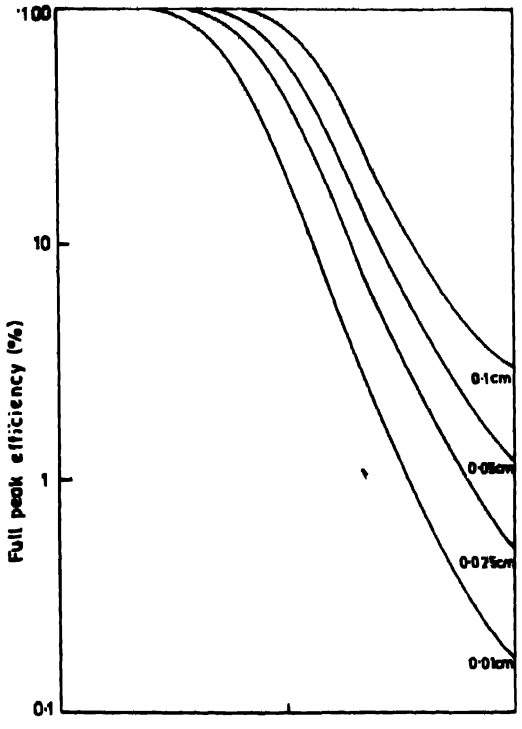

Figure 5. The full energy peak efficiency *versus* energy curves for α-HgI_2 detectors of different thicknesses.

that the hole trapping length in α-HgI_2 single crystals is about 0.1 cm which is comparable to the thickness of the thick detectors. So as the thickness increases, hole collection becomes increasingly worse and there is a degradation in the resolution of 59.54 keV peak.

Figure 7 shows the simulated spectrum of ^{137}Cs source (662 keV) with a detector of 1 mm thickness. The 662 keV peak and the Compton edge is clearly seen in the spectrum. The height of the photopeak is very low because of the low efficiency of the detector at this high energy.

5. Conclusion

From the present study we realize that the computer simulations of X- and γ-ray semiconductor detectors are useful for a number of reasons. Some of these are :

— Effects of various parameters on the overall performance of different semiconductor detectors are better understood.

— Optimal detector geometries can be determined quickly by simulation.

— Difficult or impractical-to-build detectors can be studied without actual construction.

Further, we wish to investigate the possibility of Monte-Carlo method in including various other physical effects which are at present neglected. These effects are polarization,

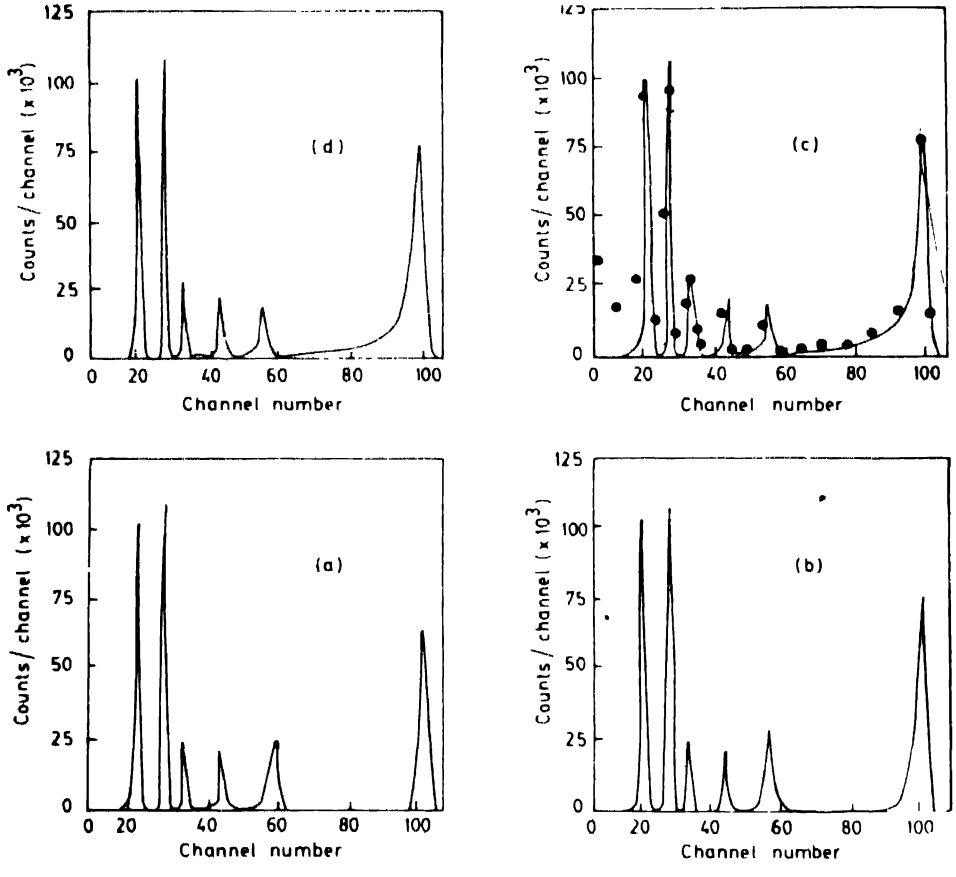

Figure 6. Simulated spectra of ^{241}Am source using α-HgI_2 detector of thicknesses (a) 0 010 cm (b) 0.025 cm (c) 0 075 cm and (d) 0.100 cm Experimental data obtained from Ref. [9] for a 500 μm thick detector is superposed on (c) by dots

nonuniform trapping of charge-carriers, charge detrapping etc. We also wish to extent this study for energies above 1 MeV

Acknowledgments

We are grateful to the Department of Atomic Energy, Government of India, for the financial assistance in the form of a research scheme. We also acknowledge the computing facilities

provided by the Computer Aided Process Engineering Laboratory of Chemical Engineering Department, Indian Institute of Technology, Kharagpur.

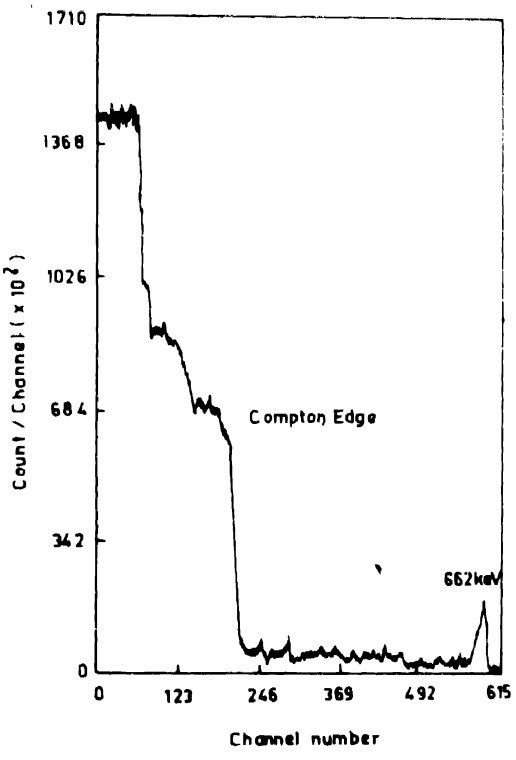

Figure 7. Simulated spectrum of ^{137}Cs source using 0 1 cm thick α-HgI_2 detector

References

[1] M Cuzin 1987 *Nucl. Instrum Meth Phys Res.* **A253** 407

[2] Z D Clayton 1967 *A Monte Carlo Calculation of the Response of Gamma-ray Scintillation Counters* in *Methods in Computational Physics* **Vol. 1** eds B Alder, S Fernbach and M Roentberg (New York · Academic)

[3] C M Davisson and R D Evans 1952 *Rev Mod Phys* **24** 79

[4] W Bambynek, B Crasemann, R W Fink, A Freund, H Mark, C D Swift, R E Price and P V Rao 1972 *Rev Mod. Phys.* **44** 716

[5] D E Raeside 1976 *Phys Med. Biol.* **21** 181

[6] G Knop and W Paul 1965 *Alpha, Beta and Gamma Spectroscopy* ed K Siegbahn (Amsterdam North-Holland)

[7] R B Day, G Dearnaley and J M Palms 1967 *IEEE Trans Nucl Sci.* **NS-14** 487

[8] G F Knoll 1989 *Radiation Detection and Measurement* (New York · John Wiley) 2nd edn

[9] J S Iwanczyk, J S Kusmiss, A J Dabrowski, J B Barton, G C Huth, T E Economou and A L Turkevich 1982 *Nucl. Instrum Meth.* **193** 73